Supplementary Information

Simple Preparation of Ag-BTC-Modified $Co_3Mo_7O_{24}$ Mesoporous Material for Capacitance and H_2O_2-Sensing Performances

Lijie Xu,[a] Xinyu Zhao,[a] Kai Yu,*[ab] Chunmei Wang,[a] Jinghua Lv,[a] Chunxiao Wang[a] and Baibin Zhou*[ab]

[a]Key Laboratory for Photonic and Electronic Bandgap Materials, Ministry of Education, Harbin Normal University, Harbin 150025, P.R. China

[b]Key Laboratory of Synthesis of Functional Materials and Green Catalysis, Colleges of Heilongjiang Province, Harbin Normal University, Harbin 150025, P.R. China

Experimental Section

Synthesis of Ag-BTC

$AgNO_3$ (0.28 g, 1.332 mmol) and H_3BTC (0.14 g, 0.6667 mmol) were mixed and ground with 3~5 kg force for 40 min.The obtained material was washed three times with ethanol and distilled water, and dry in 60 ℃ vacuum oven to obtain the white compound Ag-BTC.

Synthesis of $Co_3Mo_7O_{24}$

Dissolve $Co(NO_3)_2 \cdot 6H_2O$ (0.30 g, 1.03 mmol) and $(NH_4)_6Mo_7O_{24} \cdot 4H_2O$ (0.425g, 0.34 mmol) in 10 mL distilled water, the pH was adjusted to 4 with 1 M NaOH and stirred for 5 hours. The obtained material was washed with ethanol and distilled water for three times respectively. The compound was dried in a vacuum oven at 60 ℃ to obtain a light pink powder $Co_3Mo_7O_{24}$.

Synthesis of physical mixtures

Ag-BTC (0.2624 g, 1mmol) and $Co_3Mo_7O_{24}$ (0.6165g, 0.5mmol) were mixed evenly according to the ratio of {$Co_3Mo_7O_{24}$}@Ag-BTC-2 to get the physical mixture of pink-white.

Preparation of nickel foam (NF) electrode

The NF of 1×3 cm^2 was immersed in acetone and 3 M HCl for 30 minutes respectively. Wash with distilled water and ethanol and dry in a vacuum oven. The active substance, acetylene black and polyvinylidene fluoride (PVDF) were evenly mixed at a mass ratio of 8:1:1, and about 5 mg of slurry was applied to the 1 × 1 cm^2 NF. After the slurry was completely dried, the NF was pressed into 3 s by pressing machine at 3 MPa pressure.

Preparation of carbon cloth (CC) electrode

The carbon cloth of 1×3 cm^2 was immersed in acetone, distilled water and ethanol for 20 min respectively, and then placed in a vacuum oven to dry. The active substance, acetylene black and PVDF were evenly mixed at a mass ratio of 8:1:1. The slurry of about 5 mg was applied at 1 × 1 cm^2 CC, after the slurry was completely dried, a drop (7 mL) of Nafion was dripped on top, and the CC was placed in a 60 ℃ oven to dry overnight.

Preparation of glassy carbon electrode (GCE)

The active material and acetylene black were mixed at a mass ratio of 1:3 and ground in an agate mortar to a fine powder. The sample (5 mg) was mixed with ethanol and then 7 mL was taken by using a liquid transfer gun and added to the GCE. After the sample is completely dried, add another drop of Nafion and set aside.

Preparation of symmetrical double electrode

In a symmetrical double electrode system, a symmetrical supercapacitor (SSC) was assembled with {$Co_3Mo_7O_{24}$}@Ag-BTC-2-NF as positive and negative electrodes placed on both sides of the isolation plate in a 1 M Na_2SO_4 electrolyte. The weight of the two NF electrodes is roughly the same.

Characterization methods

All of the chemicals in work were purchased from commercial sources and used without further purification. Infrared (IR) was recorded in the range 400-4000 cm^{-1} on an Alpha Centaurt FTIR spectrophotometer with pressed KBr pellets. The powder X-ray diffraction (XRD) information was obtained on a Bruker AXS D8 Advance instrument with Cu-Kα radiation (λ=1.5418Å) in the 2θ range of 5-60°. Morphology analysis of the this material was collected on a JEOL JSM-6700 M scanning electron microscope (SEM). Transmission electron microscopy (TEM) image was taken on a Hitachi H-800 transmission electron microscope. The chemical composition was studied by X-ray photoelectron spectroscopy (XPS) using a Thermo Scientific X-ray photoelectron (K-alpha). The nitrogen adsorption-desorption analysis at 77 K could estimate the specific surface area and pore size distribution of the sample from Tristar 3020 Brunauer-Emmett-Teller (BET) Micrometrics. The Diamond 6300 thermogravimetric(TG) analyzer manufactured by Perkin Elmer was used to test the change of sample weight with temperature or time. Shimazu Instruments UV-2700 UV analyzer was used to test the wavelength range of 200-800 nm. The ICP analyzer was performed in ICP-MS:Aglient 7800 analyzer.

Calculation formula

Three electrode specific capacitance:

$$C_s = I \times \Delta t/(m \times \Delta V) \qquad (1)$$

where C_s is the specific capacitance, *I* is the current during discharge, (*I/m* is the current density during discharge), *Δt* means the time of discharge, *m* is the mass of the electrode materials, and *ΔV* is the voltage difference between the upper and lower potential limits.

Dynamics:

$$i = av^b \qquad (2)$$

Where *i* is the peak current density (in CV curve), *v* is the scanning rate, *a* and *b* is the coefficient.

$$Q = Q_c + Q_d \qquad (3)$$

Where *Q* is the amount of charge, Q_c is the control charge and Q_d is the diffusion charge.

$$Q = Q_C + kv^{-1/2} \qquad (4)$$

Where *Q* is the total charge stored, Q_c is the control charge, *k* is the variable parameter, and *v* is the scanning rate.

Specific capacitance of symmetrical double electrode:

$$C = 2I \times \Delta t/(m \times \Delta V) \qquad (5)$$

Energy density and power density:

The energy density (*E, Wh* kg^{-1}) and power density (*P, W* kg^{-1}) are calculated by the constant current discharge curve using the following formula:

$$E = C_s \Delta V^2/7.2 \qquad (6)$$

$$P = E \times 3600/t \qquad (7)$$

Where C_s, *ΔV* and *t* are the total capacitance, the voltage difference between the upper and lower potential limits and discharge time of the symmetric supercapacitor.

Calculate the catalytic efficiency according to the following expression:

$$CAT = 100\% \times [Ip\{compound\}H_2O_2 - Ip\{compound\}]/Ip\{compound\} \qquad (8)$$

$Ip\{compound\}H_2O_2$ and *Ip{compound}* represent the peak oxidation current of the compound with and without H_2O_2 respectively.

Results and discussion

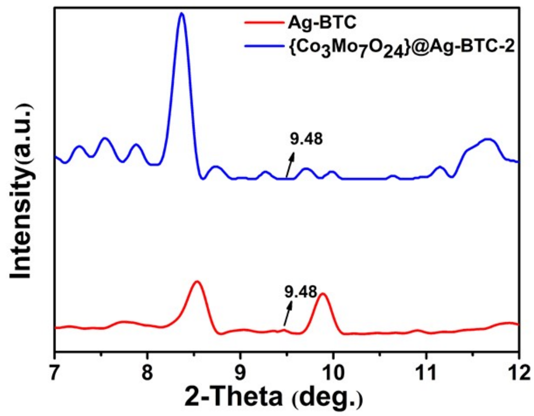

Fig. S1 Part XRD patterns of Ag-BTC and $\{Co_3Mo_7O_{24}\}$@Ag-BTC-2.

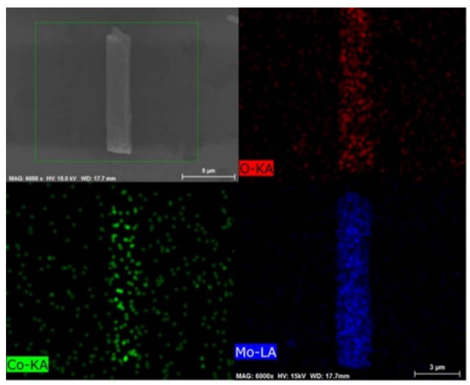

Fig. S2 SEM and EDX of $Co_3Mo_7O_{24}$.

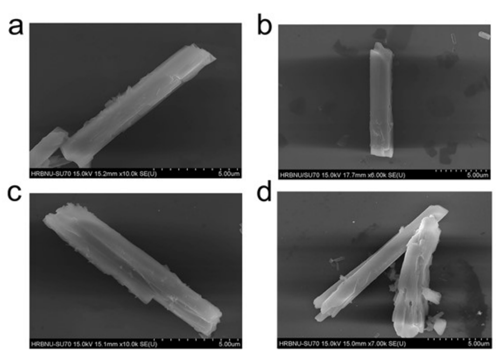

Fig. S3 The SEM of (a) Ag-BTC, (b) $Co_3Mo_7O_{24}$, (c) $\{Co_3Mo_7O_{24}\}$@Ag-BTC-2 and (d) physical mixture.

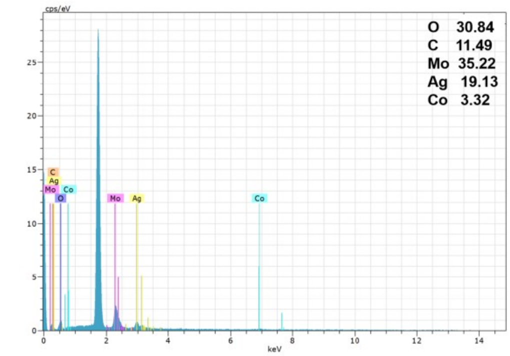

Fig. S4 EDS of $\{Co_3Mo_7O_{24}\}$@Ag-BTC-2.

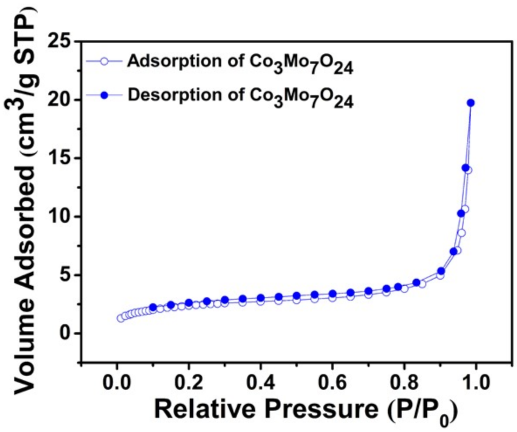

Fig. S5 N_2 adsorption-desorption isotherms of $Co_3Mo_7O_{24}$.

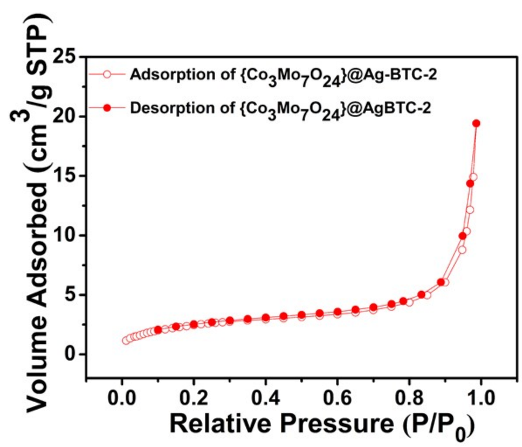

Fig. S6 N_2 adsorption-desorption isotherms of $\{Co_3Mo_7O_{24}\}$@Ag-BTC-2.

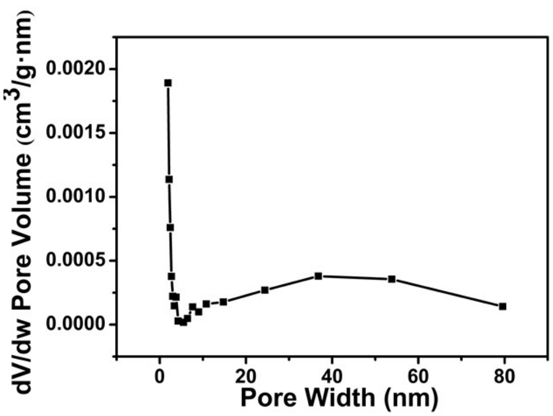

Fig. S7 Pore size diagram of $Co_3Mo_7O_{24}$.

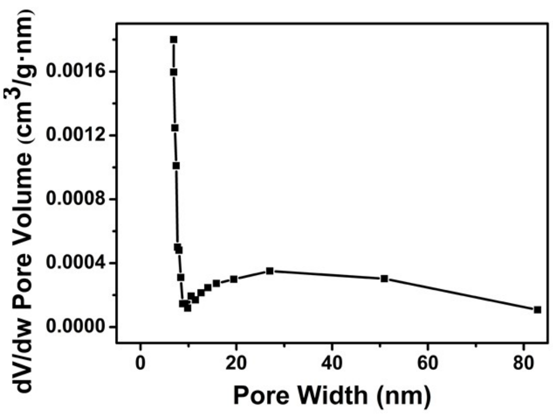

Fig. S8 Pore size diagram of $\{Co_3Mo_7O_{24}\}$@Ag-BTC-2.

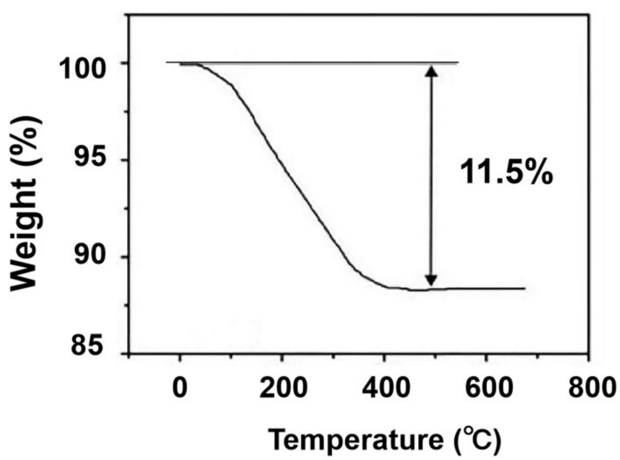

Fig. S9 TG curve of $\{Co_3Mo_7O_{24}\}$@Ag-BTC-2.

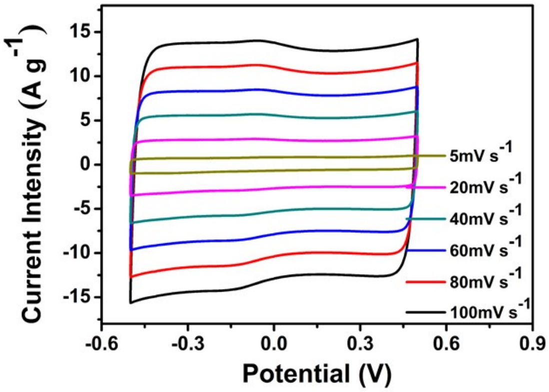

Fig. S10 The CV curves of $Co_3Mo_7O_{24}$ at different scaning rate with NF as the collector.

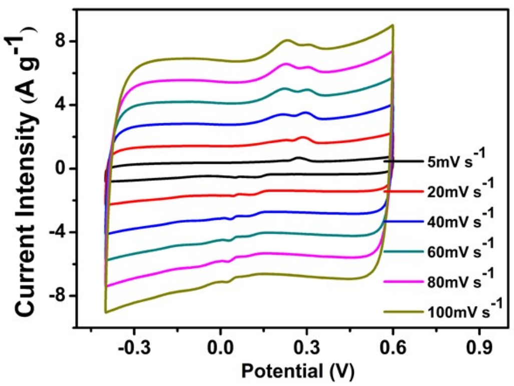

Fig. S11 The CV curves of Ag-BTC at different scaning rate with NF as the collector.

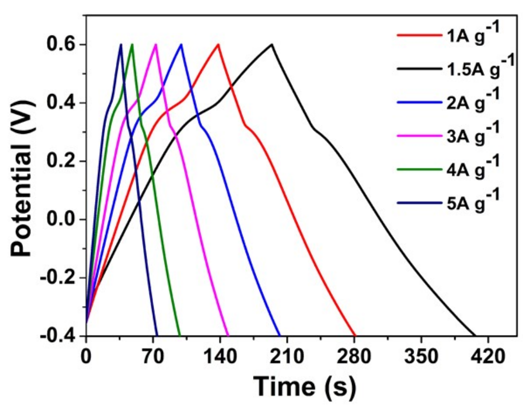

Fig. S12 The GCD curves of $Co_3Mo_7O_{24}$ at different current densities with NF as the collector.

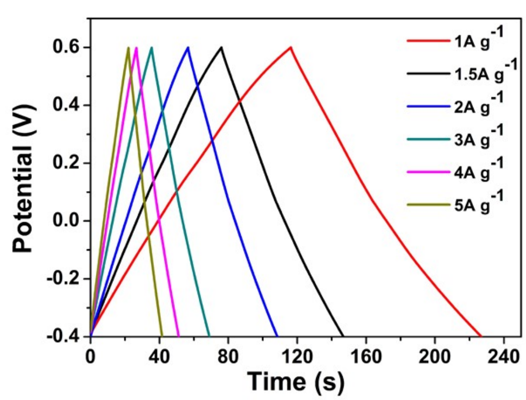

Fig. S13 The GCD curves of Ag-BTC at different current densities with NF as the collector.

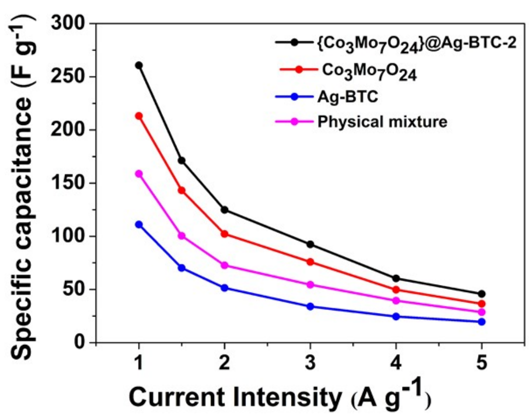

Fig. S14 The specific capacitance of four materials at various current densities.

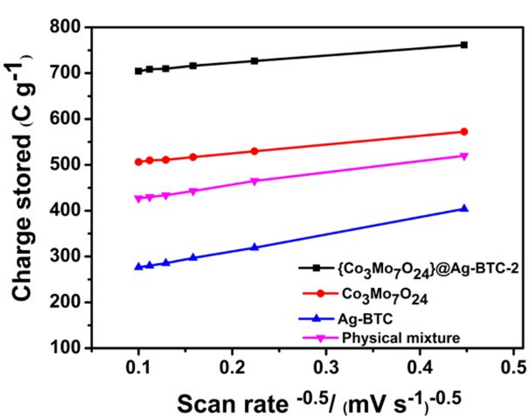

Fig. S15 The total charge stored of four materials.

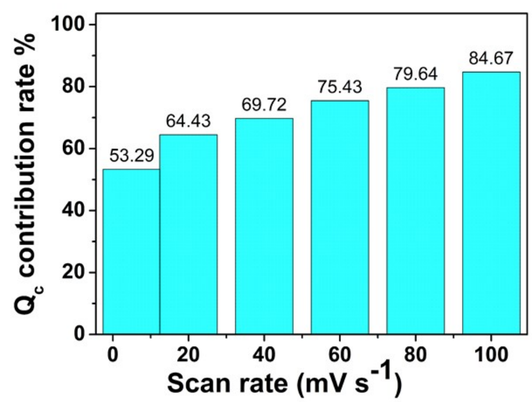

Fig. S16 Contribution ratio of Q_c of $Co_3Mo_7O_{24}$ at various scan rates with NF as the collector.

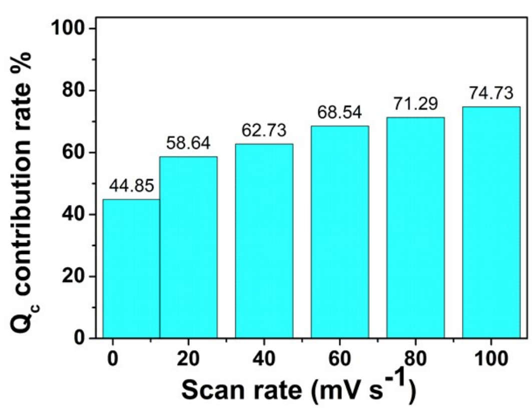

Fig. S17 Contribution ratio of Q_c of Ag-BTC at various scan rates with NF as the current collector.

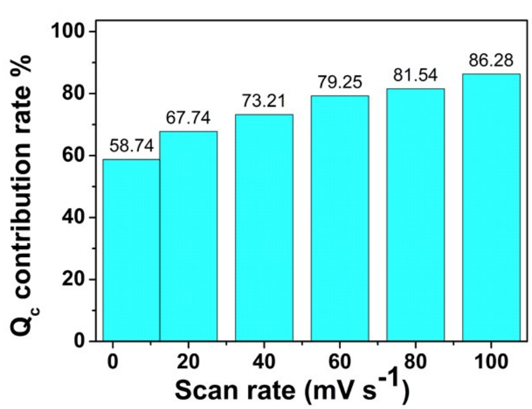

Fig. S18 Contribution ratio of Q_c of physical mixture at various scan rates with NF as the collector.

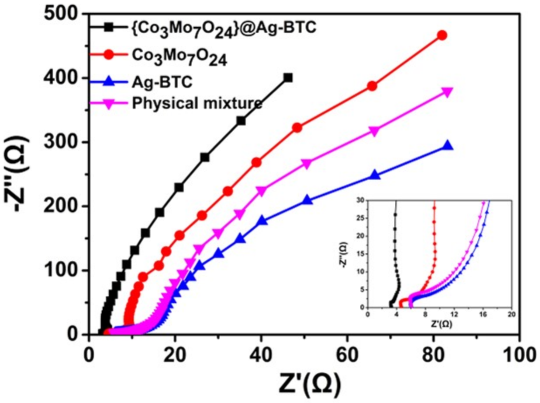

Fig. S19 The EIS of four materials after 5000 cycles with NF as the collector.

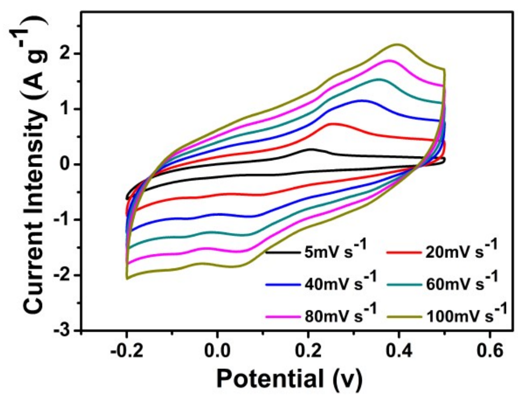

Fig. S20 The CV curves of $\{Co_3Mo_7O_{24}\}$@Ag-BTC-2 at different scaning rate with CC as the collector.

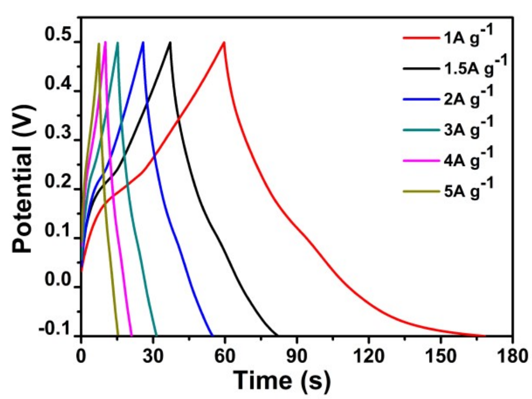

Fig. S21 The GCD curves of $\{Co_3Mo_7O_{24}\}$@Ag-BTC-2 at different current densities with CC as the collector.

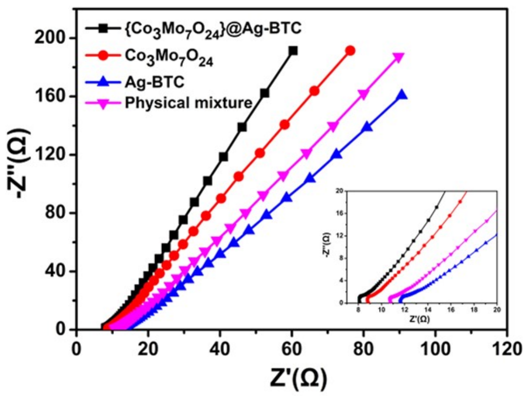

Fig. S22 The EIS of four materials after 5000 cycles with CC as the collector.

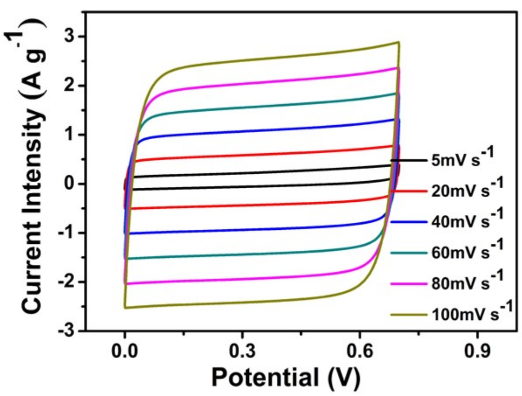

Fig. S23 The CV curves of $\{Co_3Mo_7O_{24}\}$@Ag-BTC-2-NF in a symmetrical supercapacitor.

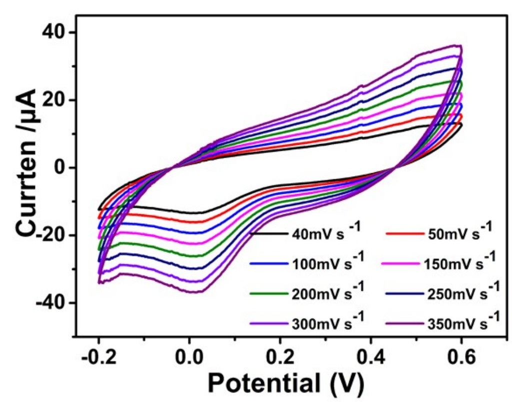

Fig. S24 The CV curves of $\{Co_3Mo_7O_{24}\}$@Ag-BTC-2-GCE at different scanning rates.

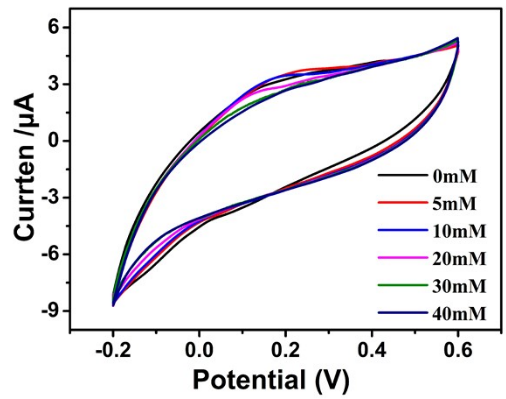

Fig. S25 The CV curve of the different concentrations of H_2O_2 of $Co_3Mo_7O_{24}$-GCE.

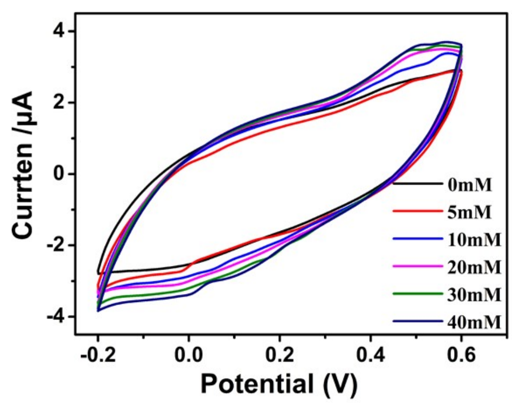

Fig. S26 The CV curve of the different concentrations of H_2O_2 of Ag-BTC-GCE.

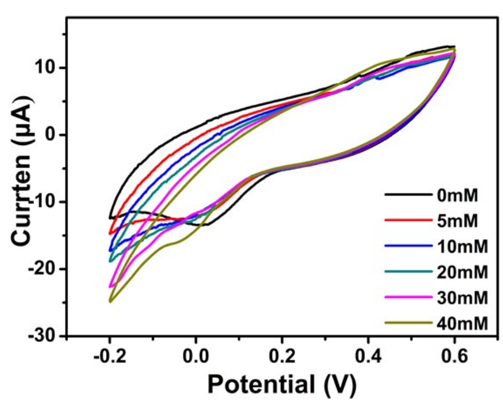

Fig. S27 The CV curve of the different concentrations of H_2O_2 of {$Co_3Mo_7O_{24}$}@Ag-BTC-2-GCE.

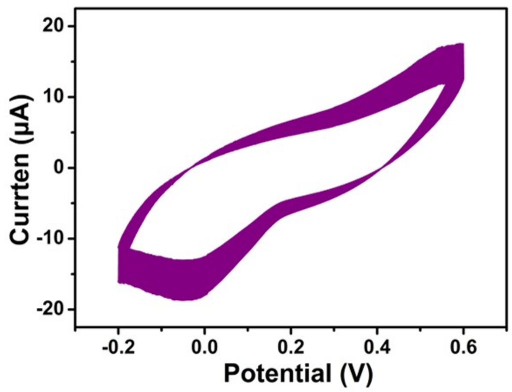

Fig. S28 The CV curve of 1000 cycles at a 50 mV s^{-1} of $\{Co_3Mo_7O_{24}\}$@Ag-BTC-2-GCE.

Table S1 Element contents (wt %) of $\{Co_3Mo_7O_{24}\}$@$[Ag_4(\mu\text{-}Hbtc)(\mu\text{-}H_2btc)]_{1/2}$ characterized by ICP-MS.

Samples	Co	Mo	Ag
$\{Co_3Mo_7O_{24}\}$@$[Ag_4(\mu\text{-}Hbtc)(\mu\text{-}H_2btc)]_{1/2}$	8.72	38.67	14.43

Table S2 Comparison of the properties of the POMs-based materials with several published supercapacitors.

materials	specific capacitance	cycling stability	current collector	Ref.
$\{Cu(3\text{-}H_2bptzpe)_2[\gamma\text{-}Mo_8O_{26}]\}$	190.3 F g^{-1} (1 A g^{-1})		carbon cloth	1
$\{Cu_2(3\text{-}bptzp)_2(H_2O)_4[\gamma\text{-}Mo_8O_{26}]\}$	263.7 F g^{-1} (1 A g^{-1})		carbon cloth	1
MF POMs/MXenes (Fe^{3+} and $[Mo_7O_{24}]^{6-}$ ions for synthesizing MF POMs)	627 mA h g^{-1} (0.1 A g^{-1})	75.3% (1000 cycles)		2
$AC/PW_{12}O_{40}$	254 F g^{-1} (10 mV s^{-1})	35% (30000 cycles)	Graphite rods	3
$rGO/PMo_{12}O_{40}$	276 F g^{-1} (10 mV s^{-1})	96% (10000 cycles)	Graphite roods	4
$[H(C_{10}H_{10}N_2)Cu_2][PMo_{12}O_{40}]$	287 F g^{-1} (1 A g^{-1})	81.5% (500 cycles)	glassy carbon	5
$[H(C_{10}H_{10}N_2)Cu_2][PW_{12}O_{40}]$	153.43 F g^{-1} (1 A g^{-1})	18.2% (500 cycles)	glassy carbon	5
$[Ag_5(C_2H_2N_3)_6][H_5SiMO_{12}O_{40}]$@15%GO	230.2 F g^{-1} (0.5 A g^{-1})	92.7% (1000 cycles)	glassy carbon	6
$[Ag_5(C_2H_2N_3)_6][H_5SiMo_{12}O_{40}]$	155.0 F g^{-1} (0.5 A g^{-1})	78.5% (1000 cycles)	glassy carbon	6
$[Ag_5(C_2H_2N_3)_6][H_5SiW_{12}O_{40}]$	29.8 F g^{-1} (0.5 A g^{-1})	78.3% (1000 cycles)	glassy carbon	6
$[Cu^{I}_4H_2(btx)_5(PMo_{12}O_{40})] \cdot 2H_2O$	237 F g^{-1} (2 A g^{-1})	92.5% (1000 cycles)	glassy carbon	7
$[Cu^{I}_4H_2(btx)_5(PW_{12}O_{40})_2] \cdot 2H_2O$	100 F g^{-1}	90%	glassy carbon	7

	(2 A g^{-1})	(1000 cycles)		
$[Cu^{II}Cu^{I}_3(H_2O)_2(btx)_5(PW^{VI}_{10}W^{V}_2O_{40})]\cdot 2H_2O$	82.1 F g^{-1} (2 A g^{-1})	100% (1000 cycles)	glassy carbon	7
$[Cu^{I}_6(btx)_6(PW^{VI}_9W^{V}_3O_{40})]\cdot 2H_2O$	76.4 F g^{-1} (2 A g^{-1})	100% (1000 cycles)	glassy carbon	7
$[Cu^{II}Cu^{I}_3(btx)_5(SiMo^{VI}_{11}Mo^{V}O_{40})]\cdot 4H_2O$	138.4 F g^{-1} (2 A g^{-1})	97% (1000 cycles)	glassy carbon	7
$[Ag_{10}(trz)_8][HVW_{12}O_{40}]$	93.5 F g^{-1} (1.5 A g^{-1})	59.2% (750 cycles)	glassy carbon	8
$[Ag_{10}(trz)_6][SiW_{12}O_{40}]$	47.8 F g^{-1} (1.5 A g^{-1})	90.9% (1000 cycles)	glassy carbon	8
$[Ag(trz)][Ag_{12}(trz)_9][H_2BW_{12}O_{40}]$	42.9 F g^{-1} (1.5 A g^{-1})	86.5% (1000 cycles)	glassy carbon	8
$H_3PW^{VI}_{12}O_{40}\cdot(BPE)_{2.5}\cdot 3H_2O$	49.2 F g^{-1} (2 A g^{-1})	80.4% (1000 cycles)	glassy carbon	9
$H_3PMo^{VI}_{12}O_{40}\cdot(BPE)_{2.5}\cdot 3H_2O$	137.5 F g^{-1} (2 A g^{-1})	92.0% (1000 cycles)	glassy carbon	9
$L_{0.5}[Cu_2L_{3.5}(SiW_{12}O_{40})]$	159.2 F g^{-1} (3 A g^{-1})		glassy carbon	10
$[Cu^{I}(btx)]_4[SiW_{12}O_{40}]$	110.3 F g^{-1} (3.0 A g^{-1})	87% (1000 cycles)	glassy carbon	11
$[\{Cu^{I}_6(btx)_7(H_2O)_{12}\}H_4\subset(W_{12}O_{40})_2]\cdot 12H_2O$	50.0 F g^{-1} (3 A g^{-1})	87.5% (1000 cycles)	glassy carbon	11
$[Cu^{I}H_2(C_{12}H_{12}N_6)(PMo_{12}O_{40})]\cdot[(C_6H_{15}N)(H_2O)_2]$	249.0 F g^{-1} (3 A g^{-1})	93.5% (1000 cycles)	glassy carbon	12
NENU-5/PPy-0.15	1879 mF cm^{-2} (25 mA cm^{-2})		Carbon cloth	13
AC/P_2Mo_{18}	275 F g^{-1} (6 A g^{-1})	70% (2000 cycles)	Stainless steel wire mesh	14
NENU-5/PPy/60//FeMo/C	2034.51 mF cm^{-2} (2 mA cm^{-2})	80.62% (10000 cycles)	carbon cloth	15
$PAni\text{-}PMo_{12}$	172.38 F g^{-1} (1 A g^{-1})		stainless steel	16
$\{Ag_6Mo_7O_{24}\}$@Ag-MOF	320.8 F g^{-1} (1 A g^{-1})	98.2% 5000 cycles	nickel foam	17
$[Ag_5(brtmb)_4][VW_{10}V_2O_{40}]$	206 F g^{-1} (110 A g^{-1})	81.7% (1000 cycles)	glassy carbon	18
$\{Cu_2SiW_{12}O_{40}\}$@HKUST-1	403.7 F g^{-1} (1 A g^{-1})	91.7% (6000 cycles)	nickel foam	19
$[Co(H_2Ptep)(HPtep)(H_2O)_2(PW_{11}CoO_{39})]\cdot 4.5H_2O$	212 F g^{-1} (1 A g^{-1})	90.2% (1000 cycles)	glassy carbon	20
$[Co(H_2Ptpi)_2(HPtpi)_2(SiMo_{12}O_{40})_2]\cdot 2H_2O$	202 F g^{-1} (1 A g^{-1})	85.8% (1000 cycles)	glassy carbon electrode	20
$NiPMo_{12}$/SWNTs	815. 6 F g^{-1} (1 A g^{-1})	96.5% (6000 cycles)	glassy carbon	21
$Co^{II}(pzta)_2(H_2O)_2(H_4GeMo_{12}O_{40})\cdot 4H_2O$	121.5 F g^{-1} (1 A g^{-1})	86% (1000 cycles)	glassy carbon	22
$[Co^{II}(pzta)_2(H_2O)]_2(H_4SiMo_{12}O_{40})\cdot 4H_2O$	182.0 F g^{-1} (1 A g^{-1})	91% (1000 cycles)	glassy carbon	22
$[Mn_2(BTC)_{4/3}(H_2O)_6]_6[K_8(SiW_{10}Mn_2Cl_4O_{36})]$	211.0 F g^{-1} (1 A g^{-1})	96.0% (5000 cycles)	nickel foam	23
$[Mn_3Mo_{12}O_{24}(OH)_6(HPO_3)_8(H_2O)_6]^{4-}$	602 mA h g^{-1} (0.1 A g^{-1})	87.6% (50 cycles)	copper foil	24
$[HPMo^{VI}_9Mo^{V}_3O_{40}]Cu^{I}_5[4\text{-}atrz]_6\cdot H_2O$	231.7 F g^{-1} (1 A g^{-1})	88.2% (1000 cycles)	glassy carbon	25
$[HPW^{VI}_9W^{V}_3O_{40}]Cu^{I}_5[4\text{-}atrz]_6$	147.5 F g^{-1} (1 A g^{-1})	95.3% (1000 cycles)	glassy carbon	25
$[H_2SiMo^{VI}_9Mo^{V}_3O_{40}]Cu^{I}_5[4\text{-}atrz]_6\cdot H_2O$	232.5 F g^{-1}	98.8%	glassy carbon	25

	(1 A g^{-1})	(1000 cycles)		
$[HPMo_{12}O_{40}]@[Cu_4(\mu_2\text{-}OH)_2(C_6H_5PO_3)_2(bimb)_4]$	267.0 F g^{-1} (5 A g^{-1})	95.1% (1000 cycles)	glassy carbon	26
PW_{12}@MIL-101/PPy-0.15	1124 mF cm^{-2} (0.5 mA cm^{-2})		nickel foam	27
PW_{12}@MIL-101	158 mF cm^{-2} (0.5 mA cm^{-2})		nickel foam	27
$H_3[Cu_2(4\text{-dpye})_2\ (PMo_{12}O_{40})]$	260.0 F g^{-1} (0.5 A g^{-1})	94.6% (2000 cycles)	carbon cloth	28
$H[Cu_2(4\text{-Hdpye})_2(PMo_{12}O_{40})\ (H_2O)_4]\cdot 2H_2O$	196.6 F g^{-1} (0.5 A g^{-1})		carbon cloth	28
$[BMIM]_4SiW_{12}O_{40}$	172 F g^{-1} (7 mA cm^{-2})	89% (1100 cycles)	glassy carbon	29
$\{Co_3Mo_7O_{24}\}$@Ag-BTC-2	260.7 F g^{-1} (1 A g^{-1})	99.8% (5000 cycles)	nickel foam	This work
	181.3 F g^{-1} (1 A g^{-1})	95.2% (5000 cycles)	carbon cloth	

References

1 Y. Tian, Z. H. Chang, X. L. Wang, H. Y. Lin, Y. C. Zhang, Q. Q. Liu and Y. Z. Chen, *Chem. Eng. J.*, 2022, **428,** 132380.
2 H. X. Chao, H. Q. Qin, M. D. Zhang, Y. C. Huang, L. F. Cao, H. L. Guo, K. Wang, X. L. Teng, J. K. Cheng, Y. K. Lu, H. Hu and M. B. Wu, *Adv. Funct. Mater.*, 2021, **31,** 2007636.
3 J. Suarez-Guevara, V. Ruiz and P. Gomez-Romero, *J. Mater. Chem. A*, 2014, **2,** 1014.
4 J. Suarez-Guevara, V. Ruiz and P. Gomez-Romero, *Phys. Chem. Chem. Phys.*, 2014, **16,** 20411.
5 S. Roy, V. Vemuri, S. Maiti, K. S. Manoj, U. Subbarao and S. C. Peter, *Inorg. Chem.*, 2018, **57,** 12078.
6 Y. Hou, D. F. Chai, B. N. Li, H. J. Pang, H. Y. Ma, X. M. Wang and L. C. Tan, *ACS Appl. Mater. Interfaces*, 2019, **11,** 20845.
7 D. F. Chai, C. J. Gómez-García, B. N. Li, H. J. Pang, H. Y. Ma, X. M. Wang and L. C. Tan, *Chem. Eng. J.*, 2019, **373,** 587.
8 Y. Hou, H. J. Pang, C. J. Gómez-García, H. Y. Ma, X. M. Wang,and L. C. Tan, *Inorg. Chem.*, 2019, **58,** 16028.
9 C. L. Wang, S. Rong, Y. Q. Zhao, X. M. Wang and H. Y. Ma, *Transit. Metal Chem.*, 2021, **46,** 335.
10 J. X. Wang, L. Zhang, L. J. Zhao, T. Li and S. B. Li, *J. Mol. Struct.*, 2021, **1231,** 129966.
11 D. F. Chai, Y. Hou, K. P. O'Halloran, H. J. Pang, H. Y. Ma, G. N. Wang and X. M. Wang, *ChemElectroChem*, 2018, **5,** 3443.
12 D. F. Chai, J. J. Xin, B. N. Li, H. J. Pang, H. Y. Ma, K. Q. Li, B. X. Xiao, X. M. Wang and L. C. Tan, *Dalton Trans.*, 2019, **48,** 13026.
13 H. N. Wang, M. Zhang, A. M. Zhang, F. C. Shen, X. K. Wang, S. N. Sun, Y. J. Chen and Y. Q. Lan, *ACS Appl. Mater. Interfaces*, 2018, **10,** 32265.
14 A. Q. Mu, J. S. Li, W. L. Chen, X. J. Sang, Z. M. Su and E. B. Wang, *Inorg. Chem. Commun.*, 2015, **55,** 149.
15 Y. Z. Liu, W. Yao, H. M. Gan, C. Y. Sun, Z. M. Su and X. L. Wang, *Chem. Eur. J.*, 2019, **20,** 16617.
16 A. Manivel, A. M. Asiri, K. A. Alamry, T. Lana-Villarreal and S. Anandan, *Bull. Mater. Sci.*, 2014, **37,** 861.
17 X. Y. Zhao, L. G. Gong, C. X. Wang, C. M. Wang, K. Yu and B. B. Zhou, *Chem. Eur. J.*, 2020, **26,** 4613.
18 G. N. Wang, T. T. Chen, X. M. Wang, H. Y. Ma and H. J. Pang, *Eur. J. Inorg. Chem.*, 2017, **2017,** 5350.
19 H. Liu, L. G. Gong, C. X. Wang, C. M. Wang, K. Yu and B. B. Zhou, *J. Mater. Chem. A*, 2021, **9,** 13161.
20 C. X. Sun, J. Ying, Y. P. Zhang, L. Jin, A. X. Tian and X. L. Wang, *CrystEngComm*, 2022, **24**, 587.
21 J. L. Zhuo, Y. L. Wang, Y. G. Wang, M. Q. Xu and J. Q. Sha, *CrystEngComm*, 2022, **24,** 579.
22 S. M. Hu, K. Q. Li, X. J. Yu, Z. X. Jin, B. X. Xiao, R. R. Yang, H. J. Pang, H. Y. Ma, X. M. Wang, L. C. Tan and G. X. Yang, *J. Mol. Struct.*, 2022, **1250,** 131753.
23 Z. W. Zheng, X. Y. Zhao, L. G. Gong, C. X. Wang, C. M. Wang, K. Yu and B. B. Zhou, *J. Solid State Chem.*, 2020, **288,** 121409.
24 Y. M. Nie, S. Liang, W. D. Yu, H. Yuan and J. Yan, *Chem. Asian J.*, 2018, **13,** 1199.
25 M. L. Yang, S. Rong, X. M. Wang, H. Y. Ma, H. J. Pang, L. C. Tan and Y. X. Jiang, *ChemNanoMat*, 2021, **7,** 299.
26 S. B. Li, X. G. Tan, M. Yue, L. Zhang, D. F. Chai, W. D. Wang, H. Pan and L. L. Fan, *Chem. Commun.*, 2020, **56,** 15177.
27 T. Y. Li, P. He, Y. N. Dong, W. C. Chen, T. Wang, J. Gong and W. L. Chen, *Eur. J. Inorg. Chem.*, 2021, **2021,** 2063.
28 Q. Q. Liu, X. L. Wang, H. Y. Lin, Z. H. Chang, Y. C. Zhang, Y. Tian, J. J. Lu and L.Yu, *Dalton Trans.*, 2021, **50,** 9450.
29 M. Ammamz and J. Fransaer, *J. Electrochem Soc.*, 2011, **158,** A14.